Growth and Elemental Stoichiometry of the Ecologically-Relevant Arctic Diatom *Chaetoceros gelidus*: A Mix of Polar and Temperate

Nicolas Schiffrine [1,2]*, Jean-Éric Tremblay [1,2] and Marcel Babin [1,2]

[1] Département de Biologie, Québec-Océan, Université Laval, Québec, QC, Canada, [2] Takuvik Joint International Laboratory, CNRS (France) & Ulaval (Canada), Université Laval, Département de Biologie, Québec, QC, Canada

In the wake of modest surface blooms that occur at the onset of the growth season in the nitrogen-poor surface waters of the Beaufort Sea, subsurface chlorophyll maxima (SCM) develop and persist within the nutrient-rich halocline. Algal communities of these SCM can realize a major portion of annual net primary production and are often dominated by the widespread diatom *Chaetoceros gelidus* in coastal waters. In order to assess how changing growth conditions at the SCM may affect the biological carbon pump, grazer nutrition, and dissolved nutrient inventories across the transpolar Pacific-Atlantic conduit, the elemental stoichiometry of a *C. gelidus* strain (RCC2046) isolated from the Beaufort Sea and its response to the availability of light and different forms of nitrogen (N) were examined in the laboratory. The cells were grown in semi-continuous batch cultures at 0°C under sub-saturating (LL; 5.5 μmol photons m^{-2} s^{-1}) or saturating irradiance (HL; 200 μmol photons m^{-2} s^{-1}) and with ammonium (NH_4^+), nitrate (NO_3^-) or urea as sole N form in nutrient-replete conditions. The growth rate, cell size, maximum quantum efficiency of photosystem II (F_v/F_m) and the concentrations of chlorophyll *a* (Chl *a*), biogenic silica (Si) and particulate N, phosphorus (P), and organic carbon (C) were measured during the exponential growth phase. Despite a clear response of volumetric quotas to N form, the growth rates and elemental ratios of the cells were unaffected by N form in the two irradiance treatments. Elemental ratios were affected by light and the responses were remarkably similar to those observed for temperate diatoms. Overall, this study shows that the growth and elemental composition of *C. gelidus* in the Arctic Ocean are highly resistant to changes in nitrogen form at near-freezing temperatures and suggests that this diatom possesses the ability to remain competitive despite ongoing environmental changes.

Keywords: Arctic diatom, ammonium, nitrate, urea, light, elemental stoichiometry

1. INTRODUCTION

The Arctic Ocean is currently experiencing major and abrupt transformations caused by climate change as underscored by rapid warming and a drastic reduction in the extent of summer sea ice (Bhatt et al., 2014; Overland et al., 2014). These alterations are impacting the marine ecosystem from the bottom up by triggering changes in the productivity, biomass, and assemblage

composition of phytoplankton (Wassmann and Reigstad, 2011; Wassmann et al., 2011). According to recent observations of large-scale latitudinal gradients in the elemental stoichiometry of carbon (C), nitrogen (N), and phosphorus (P) in phytoplankton, polar environments are characterized by low C:N:P ratios relative to those observed in warm waters at low latitudes (Martiny et al., 2013a,b). With the ongoing warming and increasing availability of light resulting from sea-ice loss, C:N:P ratios in the Arctic Ocean will possibly converge toward those observed at mid latitudes, thereby altering the north polar component of global elemental cycles.

Changes in the stoichiometry of elemental C, N, P, and silica (Si) fluxes in the western Arctic may have major consequences. Due to anomalously low nitrate:phosphate and nitrate:silicate ratios in source waters of the North Pacific and large Siberian rivers, annual net primary production in the Beaufort Sea, and more generally the transpolar Pacific-Atlantic conduit, is strongly N-limited (Tremblay and Gagnon, 2009; Tremblay et al., 2015). A changing C:N ratio of organic matter synthesis would therefore modulate the efficiency of the vertical carbon pump regionally (Falkowski et al., 2003) and, concomitantly with changes in other ratios, affect the nutritional value of phytoplankton for grazers and the food web (e.g., Leu et al., 2011). These changes may either rectify or amplify the nutrient imbalance of waters that transit across the central Arctic (e.g., Tremblay et al., 2014), with cascading effects on biological productivity and elemental fluxes "downstream" (e.g., Yamamoto-Kawai et al., 2006).

Besides warming and increasing light availability, changes in the relative availability of different N forms may affect phytoplankton elemental stoichiometry. In addition to dissolved inorganic N, such as nitrate (NO_3^-) and ammonium (NH_4^+), bloom-forming diatoms are able to use some forms of dissolved organic N (DON), including urea and amino acids (Antia et al., 1991). For the coastal Beaufort Sea, Simpson et al. (2013) emphasized that urea was unusually abundant and contributed as much as ∼50% of the total N assimilated annually. As the land permafrost thaws, DON supply to coastal seas is expected to increase (Frey et al., 2007; McClelland et al., 2012). Away from estuaries, where labile riverine nutrients are readily used (e.g., Tremblay et al., 2014), increased freshwater input resulting from sea-ice melt combined with increased precipitation and an intensification of the hydrological cycle, is expected to strengthen the vertical stratification of the upper Arctic Ocean (Yamamoto-Kawai et al., 2009; Carmack et al., 2016). The main effect of this additional freshwater would be to promote a large-scale regenerative system by reducing upward NO_3^- replenishment (McLaughlin and Carmack, 2010; Ardyna et al., 2011) and the relative share of this N form in total N uptake within the euphotic zone (e.g., the *f*-ratio, *sensu* Dugdale and Goering, 1967).

The assimilation of N is considered to be more energetically efficient for NH_4^+ and urea than for NO_3^- since the latter is oxidized and eight extra electrons must be used to sequentially reduce it to nitrite and NH_4^+ (Mulholland and Lomas, 2008). The relatively high energetic costs of NO_3^- assimilation led to the common assumption that, all other things being equal, diatoms should grow fastest and exhibit a different elemental stoichiometry when NH_4^+ or urea is the sole N

form provided (e.g., Levasseur et al., 1993). While these assumptions are validated by classical physiological studies (Solomon et al., 2010; Glibert et al., 2016), the interactive effects of irradiance and different N forms on the growth and overall C:N:P:Si stoichiometry of diatoms in cold polar waters remain poorly documented.

In the cold waters of the Beaufort Sea, the strong N limitation imparted by vertical stratification and the removal of NO_3^- by denitrification in source waters of the North Pacific and in shallow sediments of the Pacific Arctic results in the presence of a productive subsurface chlorophyll *a* maximum (SCM) in coastal areas (Martin et al., 2010, 2012). These SCM occur over a wide range of depths and light intensities, rely in variable parts on NH_4^+ and urea despite the greater availability of NO_3^- and account for a substantial part of the primary production (Martin et al., 2010, 2012, 2013). Both shelf and off-shore SCM are frequently dominated by *Chaetoceros gelidus* (ex. *socialis*) and to a lesser extent other chain-forming diatoms, both in terms of cell abundance and carbon biomass (Booth et al., 2002; Balzano et al., 2012; Chamnansinp et al., 2013; Coupel et al., 2015; Crawford et al., 2018). A compilation of prior studies showed that *C. gelidus* (or *C. socialis* as previously named) ranges from the Norwegian Coast in the Atlantic sector to the coastal Beaufort Sea in the Pacific sector (Kristiansen et al., 2001; Chamnansinp et al., 2013; Coupel et al., 2015; Balzano et al., 2017; Crawford et al., 2018) and at least as far North as 79°N in Baffin Bay, where it can persist from early summer to autumn in the SCM (Booth et al., 2002). The large spatial and temporal range under which the cosmopolitan *C. gelidus* is successful makes it a good candidate for an ecologically-relevant investigation of how changing growth conditions impact the stoichiometry of individual diatom species. Given the cosmopolitan nature of *C. gelidus*, we hypothesized that it is able to maintain (1) relatively high growth rates at the low irradiance characteristic of the SCM and (2) similar growth rates and elemental compositions when growing on NO_3^-, NH_4^+, or urea at a given irradiance.

2. MATERIALS AND METHODS

2.1. Culture Conditions

The marine Arctic diatom *Chaetoceros gelidus* (Chamnansinp, Li, Lundholm & Moestrup, strain RCC2046, Roscoff Culture Collection, http://roscoff-culture-collection.org/rcc-strain-details/2046) was grown in 500 mL (1 L borosilicate Erlenmeyer flasks) sterile artificial sea water. Artificial seawater was prepared using a salt base (Berges et al., 2001) and enriched with f/2 concentration of silicate (100 μM-Si), trace metals and vitamins (Guillard, 1975). Nitrogen was supplied as either NH_4^+, NO_3^-, or urea as sole N form at 100 μM-N. In order to maximize the ecological relevance of the experiments, other growth conditions were established based on prior observations made in the coastal Beaufort Sea. The concentration of phosphate in the medium was adjusted to obtain a N:P ratio of 9:1 (11.11 μM-P), which approximates the values observed just below the winter mixed layer before the productive season begins (Simpson et al., 2008). The nutrient concentrations used here largely exceed those observed in the coastal Beaufort Sea (e.g., Simpson et al., 2008;

Tremblay et al., 2008) in order to generate enough biomass for all analyses while keeping culture volumes manageably small and avoiding the onset of nutrient limitation prior to harvest. Martin et al. (2012), who investigated the high Canadian Arctic across several regions, seasons and years, reported median irradiance values of 7.9 and 167 μmol photons m^{-2} s^{-1} at the SCM and the surface, respectively. In order to mimic conditions under the summer midnight sun, the cultures were illuminated continuously by Philips$^{\circledR}$ fluorescent tubes and attenuated by neutral-density screening (LEE$^{\circledR}$ filters: 216-White diffusion) to provide 5.5 μmol photons m^{-2} s^{-1} for the low-light treatment (LL) and 200 μmol photons m^{-2} s^{-1} for the high-light treatment (HL). Irradiance in the LL treatment corresponded to 58% of the photo-acclimation index for growth (K_E = 9.5 μmol photons m^{-2} s^{-1}), established during preliminary experiments in which *C. gelidus* was acclimated to different light intensities of the same spectral composition as used in the present experiments (**Supplementary Figure 1**). Martin et al. (2012) also found that temperature at the SCM was cold and constrained within a narrow range (median of -1.2°C, min = -1.7°C, and max = 1.9°C; excluding data from Hudson Bay). Cultures were grown at 0°C to avoid the logistical complications of working at subzero temperatures. Therefore, we applied 6 different treatments during this experiment: HL NH$_4^+$, HL NO$_3^-$, HL Urea, LL NH$_4^+$, LL NO$_3^-$, and LL Urea.

For all treatments, cultures were inoculated with 10 mL aliquots (initial concentration $\geqslant$ 25 000 cell mL^{-1}) of the same *C. gelidus* stock culture (continuous light, $\sim$30 μmol photons m^{-2} s^{-1}, 0°C, f/2 media). To avoid NO$_3^-$ carry-over into other N treatments, a second transfer was made into the same conditions (**Supplementary Figure 2**). Growth was maintained semi-constant by diluting cultures with fresh medium (**Supplementary Figure 2**) and cultures were manually mixed gently three times a day. Culture sampling was undertaken when cultures reached balanced growth (MacIntyre and Cullen, 2005) i.e., when growth rate had been stable for at least 10 generations (**Supplementary Figure 2**). Treatments were conducted in triplicate. For each replicate, triplicate subsamples were taken for each of the variable measured (**Supplementary Figure 2**). Sterile techniques were used for all culture work.

2.2. Cell Number, Volume and Growth Rate Determination

Cell abundance, volume and size (sphere-equivalent diameter) were monitored daily with a Multisizer 4 Coulter Counter (Coulter Counter Beckman$^{\circledR}$). Three consecutive counts were achieved for each replicate. Samples were bubbled before each count to break *C. gelidus* chains. Growth rate was calculated as:

$$\mu = \frac{ln(N_2 - N_1)}{t_2 - t_1} \qquad (1)$$

where N_2 is the cell concentration at time t_2 and N_1 is the cell concentration at time t_2. The cell volume (equivalent spherical volume) was calculated from a spherical formula. Based on the same counting and particle size spectrum data, the aggregate

volume of detectable particles smaller than phytoplankton (e.g., bacteria) was order of magnitudes lower than the combined volume of *C. gelidus* cells.

2.3. Fluorescence Measurement and Chlorophyll *a* Concentration

In order to assess the physiological state of the cells, the maximum energy conversion efficiency, or quantum efficiency of PSII charge separation (F$_v$/F$_m$) was measured using a Phyto-PAM fluorometer (Walz GmbH$^{\circledR}$, Effeltrich, Germany). After 15 min of dark acclimation, a 3 mL subsample was transferred into the measuring chamber and was first exposed to single-turnover non-actinic probe flashes to measure the minimum fluorescence yield (F$_0$), and then to the same probe flashes while being simultaneously exposed to a multi-turnover saturating actinic flash (500 ms; 655 nm; > 2,000 μmol photons m^{-2} s^{-1}) to measure the maximum fluorescence yield (F$_m$) (see Huot and Babin, 2010). F$_v$/F$_m$ was calculated according to the following equation:

$$F_v/F_m = \frac{F_m - F_0}{F_m} \qquad (2)$$

A blank was done using 3 mL of culture filtered through a 0.2-μm syringe filter.

The concentration of chlorophyll *a* (Chl *a*), was determined by directly injecting 1 mL of culture into 6 mL of 90% acetone and incubating in the dark for 24 h at -20°C to extract pigments. The extracts were measured on a Turner TD- 700 fluorometer (Turner Designs, Sunnyvale, California, USA) based on the acidification method (Parsons et al., 1984). A blank was assessed by injecting 1 mL of artificial sea water into 6 mL of 90% acetone. Instrument was daily calibrated with manufacturer-provided solid standard, while the instrument is routinely calibrated with pure chlorophyll *a* (Sigma-Aldrich, C6144).

2.4. Cellular Content Analysis

Samples for particulate organic carbon and particulate nitrogen were collected on pre-combusted Whatman GF/F filters, desiccated at 60°C and analyzed simultaneously using an elemental analyzer (ECS 4010, Costech Analytical Technologies Inc.) coupled to a mass spectrometer (Delta V Advantage, Thermo- Finnigan). Samples for particulate phosphorus determination were filtered on pre-combusted Whatman filters, desiccated and oxidized using the method of Solôrzano and Sharp (1980). Oxidized phosphorus (as PO$_4^{3-}$) was analyzed with standard colorimetric methods (Hansen and Koroleff, 2007) adapted for the AutoAnalyzer 3 (Bran+Luebbe). Samples for biogenic silicate (BSi) determination were collected on 0.8-μm polycarbonate filters and frozen at -20°C. Filters were thawed in the laboratory and submitted to the alkaline hydrolysis method of Paasche (1980). The hydrolyzate was analyzed for Si(OH)$_4$ with an Autoanalyser 3 (see above). The different cellular contents (X) were expressed as cell quotas (Q$_X^C$, normalized by cell abundance), volumetric quotas (Q$_X^V$, normalized by cell volume) and areal quotas (Q$_X^S$, normalized by cell surface).

2.5. Statistical Analysis

Data are reported as mean $\pm$ standard deviation (SD) or presented as boxplots that show the average, spread and extremes of the data for each treatment. More details are given in **Supplementary Figure 3**. Prior to statistical testing of differences between treatments, the normality of data distributions was checked and systematically rejected. Differences between treatments were assessed with a permutational multivariate analysis of variance (PERMANOVA), using the lmp function of the lmPerm package (Wheeler and Torchiano, 2016) in R (R Development Core Team, 2019) and considered significant at $p < 0.05$.

3. RESULTS

3.1. Growth and Elemental Composition

At a given irradiance, the growth rate (μ; d^{-1}) of *C. gelidus* did not differ among the three N forms provided and ranged from 0.12 to 0.28 d^{-1} when cultures were grown at 5.5 (LL) and 200 (HL) μmol photons m^{-2} s^{-1}, respectively (**Figure 1**, **Tables 1**, **2**). The diameter and volume of the cells increased significantly with light intensity and were significantly higher for NH$_4^+$ than for NO$_3^-$ or urea-grown cells (**Tables 1**, **2**). The maximum quantum efficiency of PSII (F$_v$/F$_m$) was high ($\sim$0.6) in all treatments indicating that the cultures were in a healthy physiological state. Values decreased slightly at HL but were unaffected by N form (**Figure 2A**, **Table 2**).

Since the responses of cellular (Q$_X^C$) and volumetric (Q$_X^V$) quotas followed nearly identical trends with respect to the different experimental treatments, only the latter is presented in **Figure 2**. Other quotas are plotted in **Supplementary Figure 5** or provided in **Supplementary Table 1** for ease of comparison with previous studies on the influence of N form. The volumetric Chl *a* quota (Q$_{Chla}^V$) was significantly affected by light, N form

and an interaction of the two factors (**Figure 2B**, **Table 2**). In all N treatments, Q$_{Chla}^V$ decreased in a similar proportion (ca. 88%) with increasing light (**Figure 2B**). Cells grown with NO$_3^-$ exhibited higher Q$_{Chla}^V$ than those grown with NH$_4^+$ and urea, with values ranging from 21.48 $\pm$ 1.01 to 18.94 $\pm$ 0.57 fg Chl *a* μm^{-3} at LL and from 2.73 $\pm$ 0.46 to 2.30 $\pm$ 0.34 fg Chl *a* μm^{-3} at HL (**Figure 2B**).

Volumetric C and N quotas (Q$_C^V$ and Q$_N^V$, respectively) were significantly affected by growth conditions. In all N treatments, both Q$_C^V$ and Q$_N^V$ decreased with increasing light (**Figures 2C,D**, **Table 2**). Although the interaction between light and N form was either not or barely significant (**Figures 2C,D**, **Table 2**), the urea treatment exhibited lower Q$_C^V$ ($\sim$13%) and Q$_N^V$ ($\sim$7%) than the NH$_4^+$ and NO$_3^-$ treatments at HL. The two quotas

TABLE 1 | Growth rates, cell diameter and volume of *C. gelidus* acclimated to NH$_4^+$, NO$_3^-$, and urea under LL (5.5 μmol photons m^{-2} s^{-1}) and HL (200 μmol photons m^{-2} s^{-1}).

Nitrogen forms	NH$_4^+$		NO$_3^-$		Urea	
	LL	**HL**	**LL**	**HL**	**LL**	**HL**
Growth rate (μ; d^{-1})	0.13 (0.01)	0.28 (0.01)	0.12 (0.002)	0.27 (0.01)	0.12 (0.01)	0.27 (0.01)
Cell diameter (μm)	7.11 (0.18)	7.72 (0.15)	6.89 (0.08)	7.35 (0.17)	7.00 (0.09)	7.33 (0.16)
Volume (μm^3)	189.00 (14.26)	241.80 (14.46)	171.43 (6.03)	208.61 (15.23)	179.93 (7.21)	207.19 (14.22)

Numbers in parentheses indicate the standard deviation (n $\geqslant$ 9).

TABLE 2 | Summary of statistical analyses relating N form, irradiance or their interaction to the growth rate (d^{-1}), cell diameter (μm), volume (μm^3), PSII maximum quantum efficiency (F$_v$/F$_m$, dimensionless), volumetric Chl *a* quota (Q$_{Chla}^V$, fg μm^{-3}), volumetric quotas (Q$_C^V$, Q$_N^V$, Q$_P^V$ and Q$_{Si}^V$; fmol μm^{-3}) and molar C:N, N:P, Si:N ratios of *C. gelidus* acclimated to NH$_4^+$ (A), NO$_3^-$ (N), and urea (U) under LL (5.5 μmol photons m^{-2} s^{-1}) and HL (200 μmol photons m^{-2} s^{-1}).

Variable	Two-way PERMANOVA			HSD Tukey *post-hoc* test	
	Light	**N form**	**Interaction**	**Light**	**N form**
Growth rate	***	ns	ns	HL > LL	–
Cell diameter	***	***	***	HL > LL	A > N = U
Volume	***	***	***	HL > LL	A > N = U
Q$_{Chla}^V$	***	**	**	HL < LL	A < N >U
F$_v$/F$_m$	***	ns	ns	HL > LL	–
Q$_C^V$	***	*	ns	HL < LL	A = N >U
Q$_N^V$	***	*	*	HL < LL	A = N > U
Q$_P^V$	**	*	**	HL > LL	A < N > U
Q$_{Si}^V$	***	ns	**	HL > LL	–
C:N	ns	ns	ns	–	–
N:P	***	ns	***	HL < LL	–
Si:N	***	ns	ns	HL > LL	–
C:Chl *a*	***	ns	*	HL > LL	–

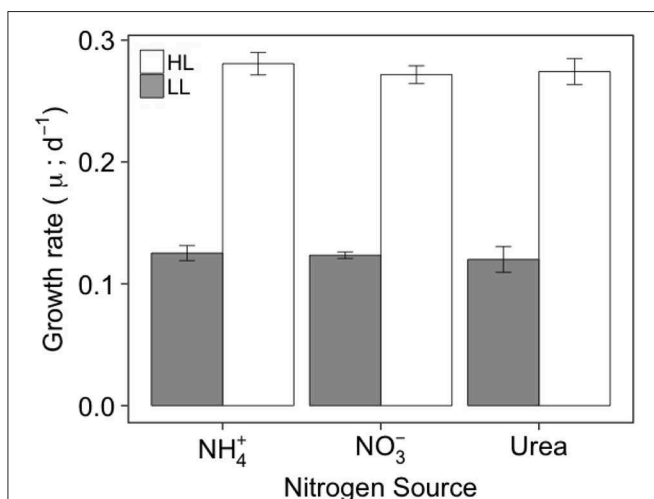*ns, p-value > 0.05; *, p-value < 0.05; **, p-value < 0.01; ***, p-value < 0.001; –indicates not tested.*

FIGURE 1 | Growth rate of *C. gelidus* acclimated to NH$_4^+$, NO$_3^-$ or urea under low (5.5 μmol photons m^{-2} s^{-1}; gray) or high (200 μmol photons m^{-2} s^{-1}; white) light at 0°C. Vertical lines indicate the standard deviation (*n* = 3).
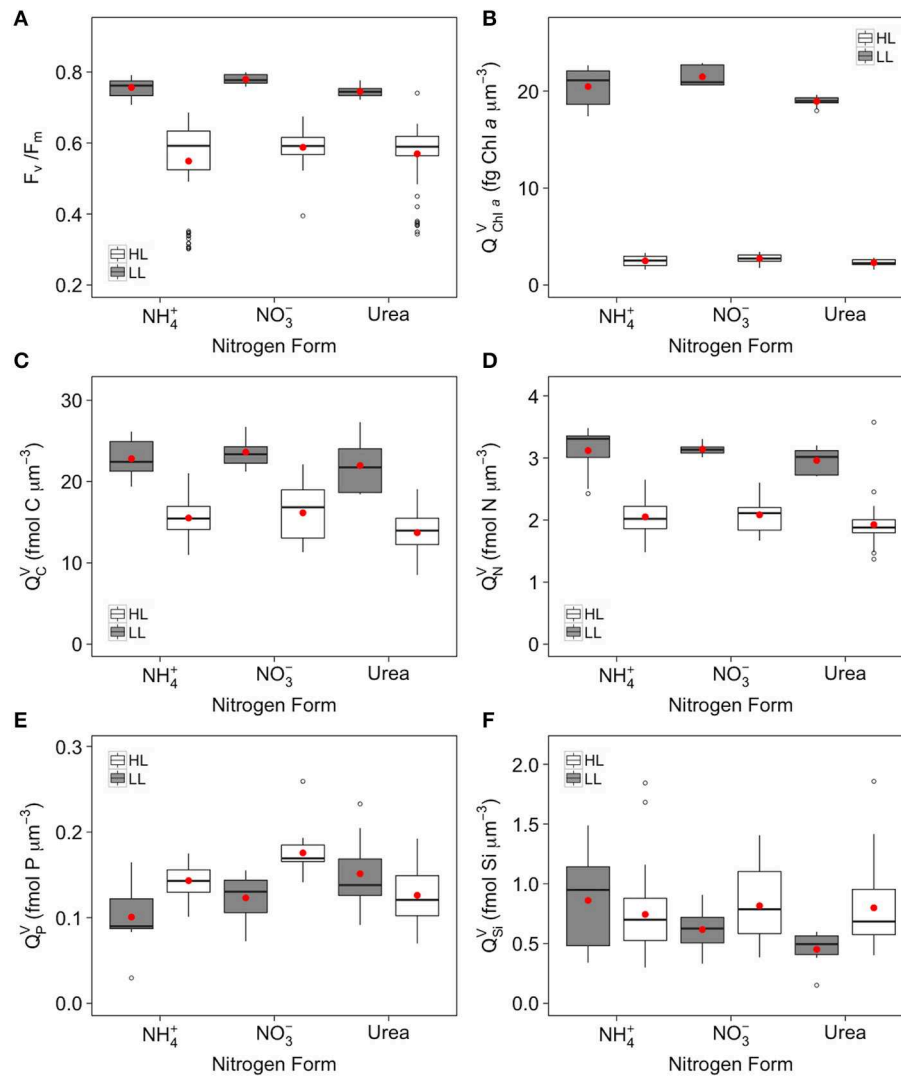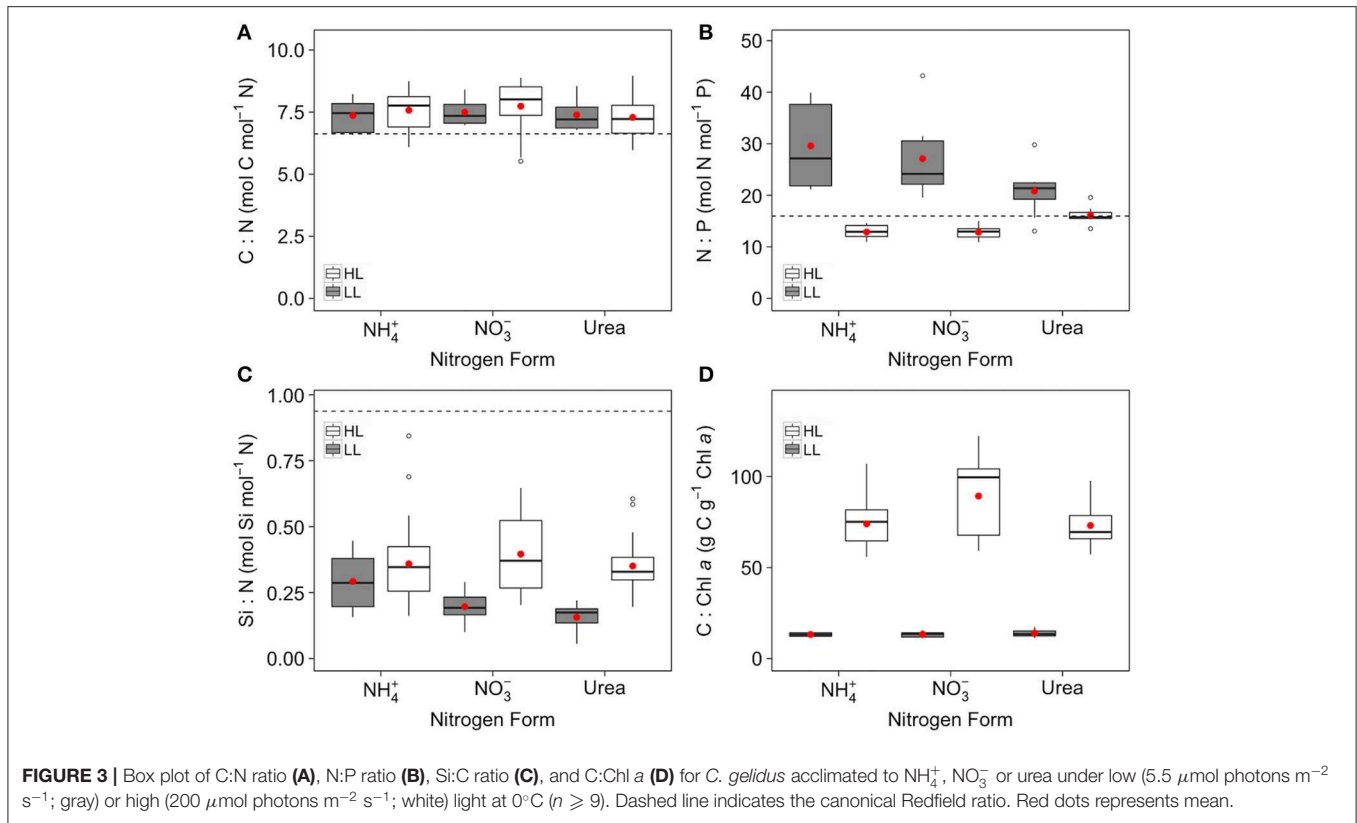
FIGURE 2 | Box plots of PSII maximum quantum efficiency (F_v/F_m) **(A)** volumetric quotas for Q^V_{Chla} **(B)**, Q^V_C **(C)**, Q^V_N **(D)** Q^V_P **(E)** and Q^V_{Si} **(F)** for cells of *C. gelidus* acclimated to NH_4^+, NO_3^- and urea under LL (5.5 μmol photons m^{-2} s^{-1}; gray) and HL (200 μmol photons m^{-2} s^{-1}; white) ($n \geqslant 9$). Red dots represent the mean.

were unaffected by N treatment at LL (**Figures 2C,D**, **Table 2**). Volumetric P quota (Q^V_P) increased with light intensity by 42% for both the NH_4^+ and NO_3^- treatments respectively (**Figure 2E**, **Table 2**), while in the urea treatment Q^V_P was similar between LL and HL (**Figure 2E**, **Table 2**). Volumetric Si quota (Q^V_{Si}) increased significantly with increasing light intensity only for NO_3^- (32%) and urea (77%) treatments, while in NH_4^+ treatment Q^V_{Si} did not significantly differ between LL and HL (**Figure 2F**, **Table 2**). At a given light intensity, Q^V_{Si} was similar unaffected by N treatment (**Figure 2F**, **Table 2**).

3.2. Elemental Ratios

The molar C:N ratio was independent of light and N form (**Figure 3A**, **Table 2**). All treatments showed a molar C:N ratio near 7.5 mol C mol^{-1} N, which was slightly higher than the Redfield value of 6.6 mol C mol^{-1} N (**Figure 3A**). The molar N:P

ratio was statistically independent of N form at a given irradiance (**Figure 3B**, **Table 2**) but decreased from LL to HL by ∼0.4-, ∼0.5-, and ∼0.8-fold for NH_4^+, NO_3^-, and urea, respectively. At HL, N:P ratios were slightly lower than Redfield (N:P = 13.7 ± 2.0 mol N mol^{-1} P; **Figure 3B**), while at LL N:P ratios largely exceeded the Redfield value in all N treatments (N:P = 25.7 ± 7.8 mol N mol^{-1} P; **Figure 3B**). The molar Si:N ratio was statistically independent of N form at a given irradiance and increased with increasing light (**Figure 3C**, **Table 2**). Although the interaction between light and N form was not significant for Si:N (**Table 2**), this ratio increased from LL to HL by ∼1.25-, ∼2-, and ∼2.25-fold for NH_4^+, NO_3^-, and urea, respectively. Molar Si:N ratios were constantly lower than the Redfield-Brzezinski average (i.e., 0.94 mol Si mol^{-1} N; Brzezinski, 1985) in all treatments (averages = 0.21 ± 0.10 and 0.37 ± 0.13 mol Si mol^{-1} N at LL and HL, respectively; **Figure 3C**). The C:Chl *a*

FIGURE 3 | Box plot of C:N ratio **(A)**, N:P ratio **(B)**, Si:C ratio **(C)**, and C:Chl *a* **(D)** for *C. gelidus* acclimated to NH_4^+, NO_3^- or urea under low (5.5 μmol photons m^{-2} s^{-1}; gray) or high (200 μmol photons m^{-2} s^{-1}; white) light at 0°C ($n \geqslant 9$). Dashed line indicates the canonical Redfield ratio. Red dots represents mean.

ratio rose significantly with light intensity, with those cultures growing at HL exhibiting values ∼6-fold higher than those at LL, and was slightly affected by N form, with cells grown on NH_4^+ exhibiting high C:Chl *a* ratios relative to those grown on NO_3^- or urea (**Figure 3D**, **Table 2**).

4. DISCUSSION

The elemental composition of microalgae is a cornerstone of marine biogeochemical fluxes and ecosystem models. Changing C:N:P:Si composition can have significant repercussions for how energy and organic matter are routed through pelagic ecosystems and exported toward the deep ocean. Yet studies of the effect of environmental change on the elemental stoichiometry of phytoplankton isolated from the Arctic are scarce despite a growing interest in the ecophysiology of polar diatoms. Two major ways in which the elemental stoichiometry of organic matter can be affected by changes in growth conditions include modifications in the physiology of microalgae and shifts in their assemblage composition. Addressing these two components simultaneously with field experiments or laboratory studies is highly challenging. Here we partially circumvented this difficulty by working with a species that will in all likelihood persist through change. The cosmopolitan species *Chaetoceros gelidus* has been abundant in the SCM communities of several sectors of the Arctic for the past 20 years certainly and possibly since the early twentieth century at least (Grøntved and Seidenfaden, 1938; Chamnansinp et al., 2013). Because the same species can

be found in northern temperate regions as well (see geographic distribution in Chamnansinp et al., 2013), there is no reason to expect that it will be displaced by competitors.

While previous studies focused solely on the effects of light intensity or temperature on Arctic diatom species (see references in Lacour et al., 2017), a comprehensive understanding of how phytoplankton will respond to changes in the generally strongly N-limited waters of the Arctic can be gained by considering N form as an additional variable. To our knowledge, this study provides the first investigation of the physiological and compositional response of a widespread diatom that qualifies as a long-term resident of the Arctic and a likely survivor of future change. An attempt was made to maximize the ecological relevance of the experiments by focusing on the environmental variables that exhibit the largest fluctuations in the area from which *C. gelidus* was isolated and to approximate the daily irradiance regime (constant lighting) and subsurface dissolved N:P ratios that prevail in the coastal Beaufort Sea during summer (Martin et al., 2012; Simpson et al., 2013). The choice of a fixed temperature of 0°C for all the experiments was based on the work of Martin et al. (2010, 2012), who investigated SCMs of the high Canadian Arctic across several regions, seasons, and years, to find that temperature at the SCM is constrained within a narrow range (−1.7 to 1.9°C). By contrast, at the SCM, irradiance levels ranged two orders of magnitude while the relative contribution of ambient NH_4^+ to the sum of NH_4^+ and NO_3^- ranged from 0.3 to 100% (Martin et al., 2012). In the present study, cultures were grown under high nutrient concentrations (see section Materials

and Methods) in order to assess the impact of irradiance and N form on actively growing cells instead of the effects of nutrient starvation on a terminating bloom. Our results and the following discussion therefore apply to nutrient-replete cells only. The effects of nutrient limitation on elemental quotas and ratios have been treated elsewhere (Geider and La Roche, 2002).

4.1. Effect of N Form on Growth Rates and Stoichiometry at Low Temperature

One paradigm for algal N nutrition stipulates that cells should achieve their highest growth rates when growing on reduced N and NH_4^+ in particular, since the cells incur a 20% incremental energy expenditure for the reduction of NO_3^- (Thompson et al., 1989; Levasseur et al., 1993). In previous studies, this expectation has been substantiated only for cells growing at saturating irradiance, possibly because the disadvantage of using NO_3^- is not manifest when growth is severely light-limited (e.g., Levasseur et al., 1993, for the temperate diatoms *Chaetoceros gracilis*). At saturating light, the lower cost of using NH_4^+ can translate into a higher growth rate and higher C, N, and chlorophyll *a* contents (Thompson et al., 1989; Levasseur et al., 1993; Shi et al., 2015).

The results presented here partly agree with previous studies in that growth rates and volumetric or cellular quotas did not differ significantly between the NH_4^+ and NO_3^- treatments at LL (**Figures 1–3**, **Tables 1**, **2**, **Supplementary Figure 5**, **Supplementary Table 1**). At HL, however, the growth rates of *C. gelidus* were also unaffected by N form. This contrast with prior studies is possibly due to the low temperature used in our study. In a parallel set of experiments in which *C. gelidus* was grown at the same HL but higher temperatures, Schiffrine et al. (in prep) obtained a μ_{max} of 0.65 d^{-1} at 6°C (**Supplementary Figure 4**). The maximum growth rates obtained here at LL and HL correspond to 20 and 43% of this μ_{max}, respectively, representing a relatively small growth increment given the 36-fold difference in irradiance between the two treatments and the fact that irradiance at LL was lower than the half-saturation constant for light at 0°C (K_E = 9.5 μmol photons m^{-2} s^{-1}; **Supplementary Figure 1**). Recently, it has been suggested that the relatively low growth rates at 0°C can be attributed to the limitation of C fixation resulting from the slow catalytic activity of Rubisco (Young et al., 2015; Lacour et al., 2018). In this context, the strong control of temperature on C fixation presumably nullifies the energetic advantage of using NH_4^+. This scenario is consistent with the invariance of Q_C^V for our *C. gelidus* cultures growing at HL and 0°C on NO_3^- or NH_4^+ (**Figure 2C**, **Table 2**). The nearly equal values of Q_{Chla}^V and F$_v$/F$_m$ in these two N treatments further suggests that cells using NO_3^- did not strain to maintain high photosynthetic capacity and offset the greater reductant requirement of N assimilation by trapping more light energy, in contrast with studies performed at relatively high temperature (Thompson et al., 1989; Levasseur et al., 1993). The lack of differences in Q_{Si}^V (**Figure 2F**, **Table 2**) or in areal Si quota (Q_{Si}^S; **Supplementary Table 1**) between the NH_4^+ and NO_3^- treatments further indicates that the lower energetic cost of using NH_4^+ had no positive impact on the inclusion of silicon in the forming frustule.

Urea assimilation is supposedly as energetically inexpensive as NH_4^+ assimilation, since the investment required to cleave urea is offset by the release of two NH_4^+ molecules (e.g., Solomon et al., 2010). This notion is supported by the lack of difference in growth rate for cells using urea and NH_4^+ at either light intensity (**Tables 1**, **2**). However, a closer look at the HL condition reveals that Q_{Chla}^V, Q_C^V, and Q_N^V for the urea treatment were substantially lower than in the NH_4^+ treatment, while F$_v$/F$_m$ Q_{Si}^V remained invariant despite a slight difference in cell size (**Figures 1–2**, **Tables 1**, **2**). These results suggest that urea-grown cells do not accumulate as much biomass as their NH_4^+-grown counterparts for reasons that remain unclear. As example, Price and Harrison (1988) observed that urea uptake and assimilation by the diatom *Thalassiosira pseudonana* was followed by the release of C and N, whereas Jauffrais et al. (2016) observed relatively high accumulations of dissolved organic C and N in the culture medium of a urea-grown benthic diatom, *Entomoneis paludosa*. The ability of the *C. gelidus* to acquire N from urea may also have been impaired by the absence of a circadian light cycle in our experiments. For cells of the temperate diatom *Thalassiosira pseudonana* grown with urea, Bender et al. (2012) observed a lesser number of transcripts for urease during the day, suggesting that most urease activity occurs at night. Using continuous lightning as we have done here to approximate mid-summer conditions at high latitudes possibly diminished urease activity and leads to lesser Q_N^V quotas and an efflux of excess C and P from the cells. This scenario implies some degree of uncoupling between urea uptake and net biomass accumulation, which cannot be confirmed here in the absence of a mass balance approach.

The relatively low elemental quotas of urea-grown cells suggest that the C production and biomass synthesis supported by urea in the ocean may prove to be less than expected from the contribution of this N form to total N uptake by microalgae during short-term incubations. The incomplete inclusion of urea-N into biomass possibly explains why C:N uptake ratios that include urea can be substantially lower than the Redfield ratio and the C:N ratio of particulate organic matter in field studies, although several other factors may contribute (e.g., Bury et al., 1995).

Despite a N form effect on cellular quotas, the effect of N form on elemental ratios was either small or not significant (**Figure 2**, **Table 2**). Comparing the results obtained in this study with a number of similar culture investigations with various species of phytoplankton illustrates that variation is mainly dependent on species and other aspects of growth conditions such as irradiance and light regime (**Table 3**). In our case, the relative invariance of elemental ratios in cells grown with different N forms suggests a balanced reorganization of the different cellular biochemical pools across the different conditions tested.

4.2. Similarities and Contrasts Between the Elemental Ratios of *C. gelidus* and Those of Other Polar or Temperate Diatoms

The C:N ratios observed here for *C. gelidus* at 0°C (7.48 ± 0.83 mol C mol^{-1} N) are at the upper bound of values reported for other polar diatoms by Lacour et al. (2017) in the −0.5 to 5°C

TABLE 3 | Summary of published studies on the effect of different N forms on the elemental stoichiometry of phytoplankton.

Species	Light level (μmol photons m^{-2} s^{-1})	Light cycle	Temperature (°C)	Nitrogen concentration (μmol L^{-1})	Effect	Source
Photosynthetic bacteria						
Cyanophytes						
Synechococcus sp. UTEX LB 2380	100	12:12	25	550	C:N ratio was 11% higher with NO_3^- than with NH_4^+	Ruan and Giordano, 2017
					No significant difference in N:P ratio with NH_4^+ and NO_3^-	
Synechococcus WH7805	15 to 250	Continuous	24	880	C:N increased with increasing light intensity and was significantly affected by light, but not by N form	Collier et al., 2012
Red lineage						
Diatoms						
Actinocyclus sp.	145	14:10	16	50	In iron replete conditions no difference was observed between NH_4^+ and NO_3^-	Muggli et al., 1996
Chaetoceros gracilis	7 –170	Continuous	18	100	At both light intensities, C:N ratio was significantly higher in was significantly higher with urea than with NO_3^- and NH_4^+	Levasseur et al., 1993
Entomoneis paludosa	90	14:10	17	400	C:N ratio was significantly higher with urea than NH_4^+ and NO_3^-	Jauffrais et al., 2016
Thalassiosira pseudonana	7 –170	Continuous	18	100	*T. pseudonana* was not able to grow with urea as sole N form and exhibited a higher C:N ratio with NO_3^- than NH_4^+ at HL. By contrast, C:N ratio was lower with NO_3^- than NH_4^+ at LL	Levasseur et al., 1993
Thalassiosira pseudonana	5 to 200	Continuous	17.5	75	C:N ratios were often highest with NO_3^- than NH_4^+ but the difference was significant only once at a low light	Thompson et al., 1989
Thalassiosira weissflogii	170	Continuous	20	50	C:N ratio was significantly higher with NO_3^- - than NH_4^+	Price, 2005
					N form (i.e., NH_4^+ and NO_3^-) had no statistically significant effect on N:P and C:P ratios	
Thalassiosira weissflogii CCMP1407	80	14:10	20	~880	No significant difference in C:N ratio with NH_4^+, NO_3^- and urea	Lomas, 2004
Dinoflagellates						
Alexandrium tamarense	350	12:12	17	6 – 100	At low N concentration no differences were noted in C:N ratio between NH_4^+, NO_3^- and urea. Under N-replete conditions C:N was highest with urea	Leong et al., 2010
Gymnodinium sanguineum	29 –170	Continuous	18	100	At both light, C:N ratio was significantly higher with urea than with NO_3^- and NH_4^+	Levasseur et al., 1993
Haptophytes						
Emiliania huxleyi	150	14:10	16	30	In iron replete conditions no difference was observed between NH_4^+ and NO_3^-	Muggli et al., 1996
Gephyrocapsa oceanica	50 – 400	12:12	20	5	No significant difference in C:N ratio between the N forms at HL and LL	Tong et al., 2016
Green lineage						
Chlorophytes						
Dunaliella tertiocela	7 –170	Continuous	18	100	No significant difference in C:N ratio between N forms at HL and LL	Levasseur et al., 1993

temperature range (average = 5.77 ± 0.52 mol C mol^{-1} N), by Garcia et al. (2018) at 2°C (average = 6.09 ± 0.59 mol C mol^{-1} N, range 5.72–6.97), and Lomas and Krause (2019) at 2°C [average = 5.99 ± 0.99 mol C mol^{-1} N, range 5.01–7.51; calculated using the dataset of Lomas and Krause (2019), for cells in exponential growth phase]. However, the C:N ratio of *C. gelidus* is remarkably close to the average reported by Sarthou et al. (2005) for temperate diatoms (7.3 ± 1.2 mol C mol^{-1} N, range 5.0 to 9.7 mol C mol^{-1} N) and suggests that this species is able to incorporate more C per unit N in its biomass than most other Arctic diatoms. Based on the analysis of Yvon-Durocher et al. (2015), differences in experimental growth temperatures are unlikely to be the main explanation for the difference in C:N ratio between polar and temperate isolates. A combination

of interspecific variability and, possibly, different degrees of adaptation of the algae to their original growth environment is more likely. The lack of relationship between irradiance and the C:N ratio of *C. gelidus* suggest that the results of Macintyre et al. (2002) for temperate phytoplankton extend to polar ones as well.

Remarkably, values of the Si:N ratio for *C. gelidus* were much lower (0.21 ± 0.10 and 0.37 ± 0.13 mol Si mol^{-1} N at LL and HL, respectively) than those obtained for three *Thalassiosira* species isolated from the Arctic (0.70 ± 0.15 mol Si mol^{-1} N; Lomas and Krause, 2019) and for a variety of temperate or low-latitude species (0.8 ± 0.3 mol Si mol^{-1} N; Brzezinski, 1985; Sarthou et al., 2005). The contrast is even more striking when considering the Southern Ocean, where the largest and most silicified diatoms thriving near the surface or at the SCM can have Si:N ratios in excess of 4 (Hoffmann et al., 2007; Baines et al., 2010; Assmy et al., 2013). Baines et al. (2010) found that the cellular Si concentrations of Southern Ocean diatoms can be up to six times higher than those of warm water diatoms from the equatorial Pacific. The contrast between diatoms from the two polar regions is intriguing since both environments are characterized by low temperatures and relatively high silicate:nitrate ratios in the water (Tremblay et al., 2015). Pre-bloom silicate:nitrate ratios in the Southern Beaufort Sea range from 2 to 3 and are comparable to the ratios observed in the permanently open ocean zone of the Southern Ocean (e.g., Tremblay et al., 2002). In the former, silicate remains in large excess once nitrate has been seasonally depleted to zero at the surface (Tremblay et al., 2015). Clearly, the process by which high ambient silicate concentrations hypothetically led to the evolution of diatoms with thick shells as protection against grazers in the Southern Ocean (Assmy et al., 2013)does not seem to operate in the Pacific Arctic.

Oceanic areas prone to seasonally-enhanced haline stratification are conducive to the development of a shade flora consisting of large, heavily silicified diatoms that persist in the SCM throughout summer and drive large opal export fluxes (Kemp et al., 2000, 2006). Interestingly, *C. gelidus* shares a similar phenology although diatoms of the *Chaetoceros* genus are typically considered as boom-and-bust producers associated with short-lived spring blooms and carbon export (Tréguer et al., 2018). As example, *Chaetoceros dichaeta* produces short outbursts in the Antarctic Polar Frontal Zone. With molar Si:N ratios ranging from 0.7 to 1.7, depending on iron availability (Hoffmann et al., 2007), *C. dichaeta* is considered poorly protected against zooplankton by contrast to *Fragilariopsis kerguelensis* and is subject to intense grazing mortality (Assmy et al., 2013). How then can the small and barely silicified *C. gelidus* be so persistent and successful in Arctic SCMs? In their comprehensive study of diatoms in northern Baffin Bay, Booth et al. (2002) indicate that *C. gelidus* (then named *C. socialis*) serves as a mid-water food source for zooplankton (see also Sieracki et al., 1998) and possesses traits that alternately allow it to maintain its position in the water column, sink massively or re-seed the SCM. The small and lightly-silicified cells are presumably able to maintain good buoyancy when actively growing under the elevated nutrient concentrations that prevail at the SCM (Booth et al., 2002). Yet *C. gelidus* has several spines, including long ones unique to the species, which

can join clusters of small chains together into larger colonies when biomass reaches high levels (Chamnansinp et al., 2013). Such aggregates can form suddenly and lead to high carbon export, especially when the cells produce abundant exopolymeric gels (Kepkay et al., 1997; Booth et al., 2002). During July in northern Baffin Bay, cells of *C. gelidus* contributed up to 91 and 49% of total phytoplankton abundance and carbon, respectively, in moored sediment traps (Booth et al., 2002). Other studies conducted in the Beaufort Sea (Nadaï pers. comm.) and the Eurasian Arctic (Lalande et al., 2019), also report large contributions of *Chaetoceros* spp. in free-drifting sediment traps during summer and fall, but the assemblage composition was not resolved to species level in these studies. Finally, resting spores of *C. gelidus* are abundant at mid-depth throughout summer and potentially re-seed the SCM episodically until fall (Booth et al., 2002).

A closer investigation of elemental quotas can shed some light on the differences between *C. gelidus* and other diatoms in the Arctic and adjacent temperate water of the North Atlantic. A comparison with recently published data describing the relationships between elemental quota and cellular volume (e.g., Lomas et al., 2019) shows that *C. gelidus* stands out with respect to other polar diatoms (**Figure 4**). For C and N, the volumetric quotas (or "elemental density" in Lomas et al., 2019) of *C. gelidus* falls mid-way between those of Arctic and temperate species (**Figure 4**), whereas for Si it matches values for temperate species (**Figure 4**). This comparison shows that the low Si:N ratios of *C. gelidus* primarily result from a low investment in silification and that diatoms thriving in the Arctic have contrasted elemental densities (**Figure 2** and **Supplementary Table 1**). The similitude between *C. gelidus* and temperate diatoms is particularly intriguing since the former is considered to be a true psychrophilic (i.e., able to grow at temperatures below 15°C and exhibit maximum growth rates at temperature optima below 18°C; Morgan-Kiss et al., 2006) species adapted for growth in the Arctic (see Chamnansinp et al., 2013).

The response of the Si:N ratio to light contrasted with the literature, which typically reports decreasing values with increasing irradiance due to the elevation of Si content relative to N content at low growth rates (Brzezinski, 1985; Claquin et al., 2002). This elevation in Si content is mainly related to an increase in cell diameter or volume at low growth rates (Martin-Jezequel et al., 2000; Claquin et al., 2002). Although allometric relationships predict a decrease in cell volume with increasing growth rate for several diatom species (Sarthou et al., 2005), *C. gelidus* showed the opposite pattern, with the lowest growth rate coinciding with the lowest cell diameter, cell volume, Q_{Si}^V and Q_{Si}^S (**Tables 1**, **2**, **Figure 2**, **Supplementary Table 1**). However, the aforementioned allometric relationships were principally established with temperate phytoplankton species growing over a broad range of relatively warm growth temperatures. Our data for *C. gelidus* support the recently proposed notion that low temperature creates a unique allometric niche for diatoms (Lomas et al., 2019).

The low N:P ratios of *C. gelidus* at HL (13.73 ± 2.04 mol N mol^{-1} P) with respect to the canonical Redfield value are
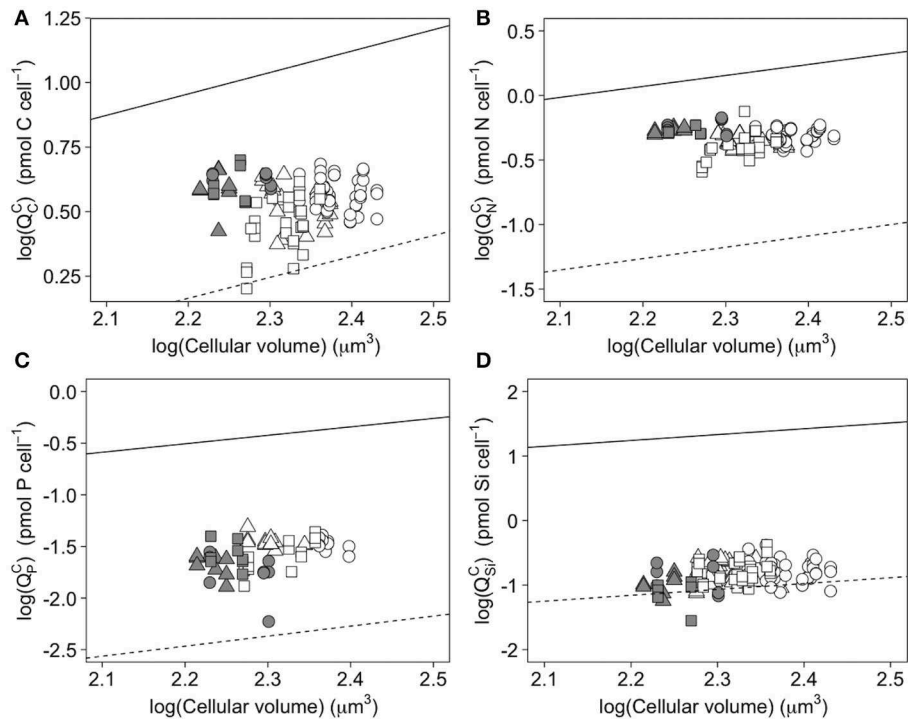
FIGURE 4 | Log-log plots of cellular elemental quotas vs. cellular volume for carbon **(A)**, nitrogen **(B)**, phosphorus **(C)**, and silicon **(D)** in *C. gelidus* cells acclimated to NH_4^+ (circles), NO_3^- (triangles) and urea (squares) under low (5.5 μmol photons m^{-2} s^{-1}; gray symbols) and high (200 μmol photons m^{-2} s^{-1}; white symbols) light at 0°C. Data are shown for all experimental replicates ($n \geqslant 9$). Allometric relationships for other polar and temperate diatoms are given by the solid and dashed lines, respectively (see references in Lomas et al., 2019).

in line with the result of Garcia et al. (2018) and Lomas et al. (2019). Both studies observed relatively low N:P ratios for polar diatoms growing at 2°C and under moderate irradiance (30–80 μmol photons m^{-2} s^{-1}). Our results and those obtained for other polar diatoms (e.g., Spilling et al., 2015; Garcia et al., 2018; Lomas et al., 2019) also fall in the range of what Sarthou et al. (2005) reported for temperate diatoms (average = 10.65 ± 3.55 mol N mol^{-1} P, range 5.00–17.90). This observation is quite intriguing, since low temperature is believed to induce low N:P ratios in phytoplankton (Toseland et al., 2013; Yvon-Durocher et al., 2015, 2017). The fact that polar diatoms grown at or near 0°C do not exhibit low N:P ratios relative to temperate diatoms growth at relatively warm temperatures suggests that the former are adapted to offset the negative effect of low temperature on N:P stoichiometry.

While the decrease in N:P ratio with increasing light and growth rate in *C. gelidus* is consistent with the growth rate hypothesis (i.e., N:P ratios decline with increasing growth rate; Sterner and Elser, 2002), the result is possibly attributable to a light effect instead of a growth response *per se*. Increases in N relative to P at low light have previously been observed and linked to an increase in N-rich proteins associated with pigment synthesis (Finkel et al., 2006). The general validity of the growth rate hypothesis is debatable in marine systems and it possibly applies best in situations where algae are P-limited (Flynn et al., 2010). P-limitation did not occur during

our study since a phosphate residual of ∼3.5 μM was observed in all treatments.

4.3. Implications for Biogeochemical Fluxes and Food Webs in the Coastal Arctic

One key result of the present study is the relatively high and constant C:N ratios that *C. gelidus* is able to maintain under contrasted irradiance levels and N forms in nutrient-replete conditions. This ability implies that this diatom accumulates more C per unit N in its biomass (+30% based on the average of Lacour et al., 2017) than most other Arctic diatoms investigated to date and is a relatively efficient exporter of carbon toward grazers and the deep ocean (Booth et al., 2002) since N is the primary limiting nutrient in the Arctic Ocean. Despite the near invariance of C:N ratios (**Figure 3**, **Table 2**), the Q_C^V and Q_N^V varied according to N form (**Figures 2C,D**, **Table 2**) and could imply changes in the nutritional quality or lability of the different components synthesized by the cells.

Both laboratory and field studies have shown that high N:P (or C:P) ratios in phytoplankton is deleterious for the growth of marine zooplankton, which may in turn have detrimental effects on the larval growth of economically valuable fish species (Elser and Hassett, 1994; Hessen et al., 2002; Leu et al., 2011). The high values observed here for the N:P (25.68 ± 7.79 mol N mol^{-1} P) and C:P (189.64 ± 51.94 mol N mol^{-1} P; **Supplementary Table 1**) ratios under LL may be suboptimal for

zooplankton growth, since the observed ratios were comparable to those considered problematic for P nutrition by Leu et al. (2011) in natural algal assemblages during late-bloom situations. However, in a future Arctic ocean where irradiance should increase, our data suggest that possible negative effects of high N:P or C:P ratios would be offset.

Despite a general warming trend of sea surface temperatures during summer, sea-ice will continue to form during the winter season. Because liquid seawater at the ice-water interface must thermodynamically be very close to its freezing point (ca. −1.8°C depending on salinity), the spring blooms that form under sea ice or when it retreats will continue to develop at near-freezing temperatures in the interior of the Arctic Ocean. The spring retreat of sea-ice is increasingly early and with the thinning of winter ice and associated reductions in snow cover, the probability that a bloom can begin under ice at subzero temperatures is increasing (e.g., Arrigo et al., 2012). In these conditions, the SCM promptly develops either before or during sea-ice retreat/melt and may drive as much as 95% of the annual new production in perennially stratified waters (e.g., Beaufort Sea; Martin et al., 2013). With the release of freshwater from melting ice and seasonal warming of the sea surface, enhanced stratification impedes the transfer of solar heat to the subsurface layer where long-lived SCM persist and *C. gelidus* thrives. This is evident in the data gathered during ArcticNet (2004–2018). At 95% of the 547 stratified stations sampled from June to October across the Beaufort Sea, the northwest passage and Baffin Bay, temperature at the SCM remained < 1°C and did not correlate with surface temperature, which ranged from −1.6 to 10.6°C (**Figure 5**; Amundsen Science Data Collection, 2018). The median temperature for all stations was 1.0°C at the SCM and 1.9°C at the surface (**Figure 5**), which remains below the optimum growth temperature of the *C. gelidus* strain used in this study (6°C; Schiffrine et al., in prep; **Supplementary Figure 4**). In this context the quantity of C that *C. gelidus* fixes per unit of the limiting nutrient (N) is expected to remain similar, thereby attenuating the impact of changing irradiance and N form on the efficiency of the biological C pump and the bulk C:N composition of the organic matter available to herbivores in coastal areas during summer.

The relatively low Si:N ratio and by extension, low Si:C ratio (**Supplementary Table 1**), observed for *C. gelidus* in our experiments under nutrient-replete conditions, suggest that SCM communities dominated by this widespread species export little Si toward deeper layers and the sediment relative to C. While it is not possible at this time to generalize this observation to other diatoms that thrive in Arctic SCMs nor to the entire year, the Si:N data for *C. gelidus* are consistent with the low particulate Si:N ratios estimated *in situ* after the end of the short-lived surface bloom in the Beaufort Sea (ca. 0.2 mol Si mol^{-1} N; Bergeron, 2013), noting that the particulate nitrogen pool may include non-diatom phytoplankton and detritus. The dominance of SCM by diatoms with low Si:N in coastal areas of the Beaufort Sea possibly contributes to the apparently low sequestration of opal in western Arctic sediments. In a budgeting exercise, Torres-Valdés et al. (2013) estimated that the export of dissolved silicate from the Arctic Ocean via Davis Strait and the western Barents Sea
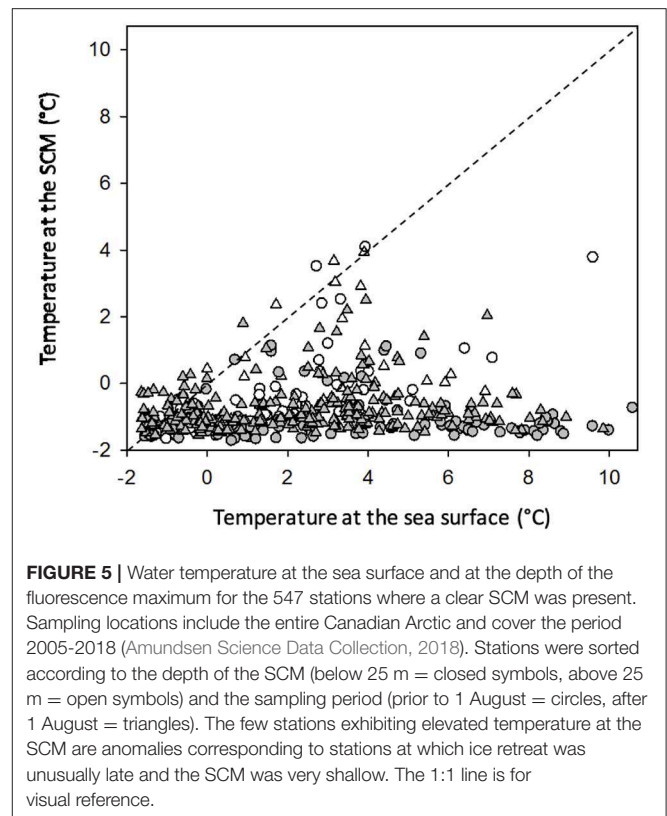

FIGURE 5 | Water temperature at the sea surface and at the depth of the fluorescence maximum for the 547 stations where a clear SCM was present. Sampling locations include the entire Canadian Arctic and cover the period 2005-2018 (Amundsen Science Data Collection, 2018). Stations were sorted according to the depth of the SCM (below 25 m = closed symbols, above 25 m = open symbols) and the sampling period (prior to 1 August = circles, after 1 August = triangles). The few stations exhibiting elevated temperature at the SCM are anomalies corresponding to stations at which ice retreat was unusually late and the SCM was very shallow. The 1:1 line is for visual reference.

Opening is roughly equivalent to the combined inputs from the shallow Bering Strait, rivers and the eastern Barents Sea Opening. Given that shallow Bering Strait is by far the largest source of silicate for the upper Arctic Ocean (Tremblay et al., 2015), the balance reported by Torres-Valdés et al. (2013) implies that very small quantities of silicon accumulate in the sediments of the Arctic Ocean and that most of the biogenic silica produced in surface waters is re-mineralized in the water column.

5. CONCLUSION

Prior studies on the elemental densities and quotas of diatoms have highlighted substantial differences based on species and size (Assmy et al., 2013; Lomas et al., 2019) and emphasized the need to resolve intra-taxon or size-based differences in order to better inform numerical ecosystem models. Yet many of the species used in culture studies aiming to close this knowledge gap continue to rely on laboratory workhorses that are easy to grow but make an undocumented contribution to early surface blooms or SCM productivity in the ocean. Setting up working cultures of the highly ecologically-relevant *C. gelidus* has proven challenging and time-consuming. For reasons that remain unknown, the cultures were lost repeatedly during the initial setting-up period when the minimum density necessary to start successful grow-out experiments was established (ca. about 25 000 cells mL^{-1}). The contrasts and similarities highlighted here in the response of *C. gelidus* vs. other diatoms isolated from the Arctic reinforce

the notion that taxa do not behave as a single entity and also underscores the need for caution when selecting species that can reasonably be used to extrapolate the results of culture studies to the real ocean.

Given its widespread distribution and frequent dominance of long-lived SCM communities across the coastal Arctic, *C. gelidus* with high C:N ratios presumably mediate an ecologically-significant portion of carbon fluxes toward grazers and the deep ocean. While the laboratory experiments performed here admittedly cannot reproduce the complexity of the natural environment, the results imply that *C. gelidus* and its biogeochemical functions in the Arctic Ocean should be resistant to variability and change in irradiance and the N form available for growth. Based on our analysis of historical data for the Beaufort Sea and Canadian Arctic, temperature at the SCM is expected to remain relatively stable by contrast with irradiance and the availability of different N forms. This stability occurs due to the isolating effect of the strong freshwater stratification, which is expected to get even stronger in the future (Nummelin et al., 2015). Since current seasonal increments of temperature in the surface layer ($+12°C$ in extreme cases, **Figure 5**) generally fail to warm the underlying SCM in the Beaufort Sea and Canadian Archipelago, projected future increases of a few degrees in mean atmospheric temperature are unlikely to be the main factor perturbating SCM communities in this sector. In this context, low temperature will likely continue to curtail the expected positive impact of greater light availability on C:N ratios and forestall secondary responses of this ratio linked to the variable energetic costs of assimilating different N forms. The situation is possibly different in the less stratified waters of the Eurasian sector of the Arctic Ocean, where changing temperature might play a much larger role.

Diatoms growing in the Southern Ocean and in the Pacific-Atlantic corridor of the Arctic Ocean all thrive in cold, Si-rich waters but show striking contrasts in their "possible" Si:N ratios. The relative contribution of giant thick-shelled diatoms vs. smaller less silicified ones is thought to control the leakage of silicate from the Southern Ocean to the North (Boyd et al., 2013). This leakage fuels the upwelling of silicate-rich water in the North Pacific, after which it moves into the Arctic interior and exits in the eastern Atlantic, mostly through Davis Strait (Torres-Valdés et al., 2013; Tremblay et al., 2015). One could imagine that diatom floristics in the Pacific-Atlantic corridor might also control the leakage of silicate into the northwest Atlantic. However, highly silicified diatoms capable of sequestering large amounts of silicon in the sediment are apparently not present or unable to strongly contribute to net primary production, allowing silicate inputs from the Bering Sea and rivers to propagate nearly unabated toward the North Atlantic (Torres-Valdés et al., 2013). A combined investigation of primary and secondary productivity, sinking fluxes and the superficial sediment would be useful to explore these ideas in the future. Our results for *C. gelidus* suggest that an increase in light availability would lead to a modest rise in Si:N ratio for cells growing on nitrate or urea and would tend to attenuate the impact of N form on this ratio.

Finally, prior culture studies have emphasized that Arctic diatoms show adaptations to their cold growth environment. The results for *C. gelidus* show that this cosmopolitan diatom shares adaptive traits with other psychrophilic diatoms, mostly through the ability to grow relatively well at low temperature. Yet it shows other characteristics that are closer to those of temperate diatoms, including relatively low volumetric elemental contents (or elemental densities) and acclimation responses to irradiance and nitrogen form. Overall, this study provides valuable insights into why *C. gelidus* is widely successful across contrasted Arctic growth environments and is seemingly equipped to handle change.

DATA AVAILABILITY STATEMENT

The datasets generated for this study are available on request to the corresponding author.

AUTHOR CONTRIBUTIONS

FUNDING

ACKNOWLEDGMENTS

SUPPLEMENTARY MATERIAL

The Supplementary Material for this article can be found online at: https://www.frontiersin.org/articles/10.3389/fmars.2019.00790/full#supplementary-material

REFERENCES

Amundsen Science Data Collection (2018). *CTD Data Collected by the CCGS Amundsen in the Canadian Arctic.* Technical report, ArcticNet Inc.

Antia, N. J., Harrison, P. J., and Oliveira, L. (1991). The role of dissolved organic nitrogen in phytoplankton nutrition, cell biology and ecology. *Phycologia* 30, 1–89. doi: 10.2216/i0031-8884-30-1-1.1

Ardyna, M., Gosselin, M., Michel, C., Poulin, M., and Tremblay, J.-É. (2011). Environmental forcing of phytoplankton community structure and function in the Canadian High Arctic: contrasting oligotrophic and eutrophic regions. *Mar. Ecol. Prog. Ser.* 442, 37–57. doi: 10.3354/meps09378

Arrigo, K. R., Perovich, D. K., Pickart, R. S., Brown, Z. W., Van Dijken, G. L., Lowry, K. E., et al. (2012). Massive phytoplankton blooms under arctic sea ice. *Science* 336, 1408. doi: 10.1126/science.1215065

Assmy, P., Smetacek, V., Montresor, M., Klaas, C., Henjes, J., Strass, V. H., et al. (2013). Thick-shelled, grazer-protected diatoms decouple ocean carbon and silicon cycles in the iron-limited Antarctic Circumpolar Current. *Proc. Natl. Acad. Sci. U.S.A.* 110, 20633–20638. doi: 10.1073/pnas.1309345110

Baines, S. B., Twining, B. S., Brzezinski, M. A., Nelson, D. M., and Fisher, N. S. (2010). Causes and biogeochemical implications of regional differences in silicification of marine diatoms. *Glob. Biogeochem. Cycles.* 24:GB4031. doi: 10.1029/2010GB003856

Balzano, S., Marie, D., Gourvil, P., and Vaulot, D. (2012). Composition of the summer photosynthetic pico and nanoplankton communities in the beaufort sea assessed by t-rflp and sequences of the 18s rrna gene from flow cytometry sorted samples. *ISME J.* 6, 1480–1498. doi: 10.1038/ismej.2011.213

Balzano, S., Percopo, I., Siano, R., Gourvil, P., Chanoine, M., Marie, D., et al. (2017). Morphological and genetic diversity of Beaufort Sea diatoms with high contributions from the *Chaetoceros neogracilis* species complex. *J. Phycol.* 53, 161–187. doi: 10.1111/jpy.12489

Bender, S. J., Parker, M. S., and Armbrust, E. V. (2012). Coupled effects of light and nitrogen source on the urea cycle and nitrogen metabolism over a diel cycle in the marine diatom *Thalassiosira pseudonana. Protist* 163, 232–251. doi: 10.1016/j.protis.2011.07.008

Bergeron, M. (2013). *Utilisation du nitrate, de l'acide silicique et du phosphate pour l'estimation de la production primaire nette et la contribution des diatomées dans l'arctique canadien (1997–2011).* Master's thesis, Université Laval, Québec, Qc, Canada.

Berges, J. A., Franklin, D. J., and Harrison, P. J. (2001). Evolution of an artificial seawater medium: improvements in enriched seawater, artificial water over the last two decades. *J. Phycol.* 37, 1138–1145. doi: 10.1046/j.1529-8817.2001.01052.x

Bhatt, U. S., Walker, D. A., Walsh, J. E., Carmack, E. C., Frey, K. E., Meier, W. N., et al. (2014). Implications of arctic sea ice decline for the earth system. *Annu. Rev. Environ. Resour.* 39, 57–89. doi: 10.1146/annurev-environ-122012-094357

Booth, B. C., Larouche, P., Bélanger, S., Klein, B., Amiel, D., and Mei, Z. P. (2002). Dynamics of *Chaetoceros socialis* blooms in the north water. *Deep Sea Res. Part II Top. Stud. Oceanogr.* 49, 5003–5025. doi: 10.1016/S0967-0645(02)00175-3

Boyd, P. W., Rynearson, T. A., Armstrong, E. A., Fu, F., Hayashi, K., Hu, Z., et al. (2013). Marine phytoplankton temperature versus growth responses from polar to tropical waters-outcome of a scientific community-wide study. *PLOS ONE* 8:e63091. doi: 10.1371/journal.pone.0063091

Brzezinski, M. A. (1985). The Si:C:N ratio of marine diatoms: interspecific variability and the effect of some environmental variables. *J. Phycol.* 21, 347–357. doi: 10.1111/j.0022-3646.1985.00347.x

Bury, S. J., Owen, N. J., and Preston, T. (1995). ^{13}C and ^{15}N uptake by phytoplankton in the marginal ice zone of the Bellingshausen Sea. *Deep-Sea Research Part II* 42, 1225–1252. doi: 10.1016/0967-0645(95)00065-X

Carmack, E. C., Yamamoto-Kawai, M., Haine, T. W., Bacon, S., Bluhm, B. A., Lique, C., et al. (2016). Freshwater and its role in the Arctic Marine System: sources, disposition, storage, export, and physical and biogeochemical consequences in the Arctic and global oceans. *J. Geophys. Res. Biogeosci.* 121, 675–717. doi: 10.1002/2015JG003140

Chamnansinp, A., Li, Y., Lundholm, N., and Moestrup, O. (2013). Global diversity of two widespread, colony-forming diatoms of the marine plankton, *Chaetoceros socialis* (syn. *C. radians*) and *Chaetoceros gelidus* sp. nov. *J. Phycol.* 49, 1128–1141. doi: 10.1111/jpy.12121

Claquin, P., Martin-Jézéquel, V., Kromkamp, J. C., Veldhuis, M. J. W., and Kraay, G. W. (2002). Uncoupling of silicon compared with carbon and nitrogen metabolisms and the role of the cell cycle in continuous cultures of *Thalassiosira pseudonana* (Bacillariophyceae) under light, nitrogen, and phosphorus control. *J. Phycol.* 38, 922–930. doi: 10.1046/j.1529-8817.2002.t01-1-01220.x

Collier, J. L., Lovindeer, R., Xi, Y., Radway, J. C., and Armstrong, R. A. (2012). Differences in growth and physiology of marine *Synechococcus* (Cyanobacteria) on nitrate versus ammonium are not determined solely by nitrogen source redox state. *J. Phycol.* 48, 106–116. doi: 10.1111/j.1529-8817.2011.01100.x

Coupel, P., Matsuoka, A., Ruiz-Pino, D., Gosselin, M., Marie, D., Tremblay, J.-É., et al. (2015). Pigment signatures of phytoplankton communities in the Beaufort Sea. *Biogeosciences* 12, 991–1006. doi: 10.5194/bg-12-991-2015

Crawford, D. W., Cefarelli, A. O., Wrohan, I. A., Wyatt, S. N., and Varela, D. E. (2018). Spatial patterns in abundance, taxonomic composition and carbon biomass of nano- and microphytoplankton in Subarctic and Arctic Seas. *Prog. Oceanogr.*. 162, 132–159. doi: 10.1016/j.pocean.2018.01.006

Dugdale, R. C., and Goering, J. J. (1967). Uptake of new and regenerated forms of nitrogen in primary productivity1. *Limnol. Oceanogr.* 12, 196–206. doi: 10.4319/lo.1967.12.2.0196

Elser, J. J., and Hassett, R. P. (1994). A stoichiometric analysis of the zooplankton-phytoplankton interaction in marine and freshwater ecosystems. *Nature* 370, 211–213. doi: 10.1038/370211a0

Falkowski, P. G., Laws, E. A., Barber, R. T., and Murray, J. W. (2003). *Phytoplankton and Their Role in Primary, New, and Export Production.* Berlin; Heidelberg: Springer, 99–121.

Finkel, Z. V., Quigg, A., Raven, J. A., Reinfelder, J. R., Schofield, O. E., and Falkowski, P. G. (2006). Irradiance and the elemental stoichiometry of marine phytoplankton. *Limnol. Oceanogr.* 51, 2690–2701. doi: 10.4319/lo.2006.51.6.2690

Flynn, K. J., Raven, J. A., Rees, T. A. V., Finkel, Z., Quigg, A., and Beardall, J. (2010). Is the growth rate hypothesis applicable to microalgae? *J. Phycol.* 46, 1–12. doi: 10.1111/j.1529-8817.2009.00756.x

Frey, K. E., McClelland, J. W., Holmes, R. M., and Smith, L. C. (2007). Impacts of climate warming and permafrost thaw on the riverine transport of nitrogen and phosphorus to the Kara Sea. *J. Geophys. Res. Biogeosci.* 112:G04S58. doi: 10.1029/2006JG000369

Garcia, N. S., Sexton, J., Riggins, T., Brown, J., Lomas, M. W., and Martiny, A. C. (2018). High variability in cellular stoichiometry of carbon, nitrogen, and phosphorus within classes of marine eukaryotic phytoplankton under sufficient nutrient conditions. *Front. Microbiol.* 9:543. doi: 10.3389/fmicb.2018.00543

Geider, R. J., and La Roche, J. (2002). Redfield revisited: variability of C:N:P in marine microalgae and its biochemical basis. *Eur. J. Phycol.* 37, 1–17. doi: 10.1017/S0967026201003456

Glibert, P. M., Wilkerson, F. P., Dugdale, R. C., Raven, J. A., Dupont, C. L., Leavitt, P. R., et al. (2016). Pluses and minuses of ammonium and nitrate uptake and assimilation by phytoplankton and implications for productivity and community composition, with emphasis on nitrogen-enriched conditions. *Limnol. Oceanogr.* 61, 165–197. doi: 10.1002/lno.10203

Grøntved, B., and Seidenfaden, G. (1938). The phytoplankton of the waters west of greenland. *Medd. Grønl.* 82, 1–380.

Guillard, R. R. L. (1975). *Culture of Phytoplankton for Feeding Marine Invertebrates.* Boston, MA: Springer, 29–60.

Hansen, H. P., and Koroleff, F. (2007). "Determination of nutrients," in *Methods of Seawater Analysis*, eds K. Grasshoff, K. Kremling, and M. Ehrhardt (Wiley-VCH Verlag GmbH), 159–228. doi: 10.1002/9783527613984.ch10

Hessen, D. O., Færøvig, P. J., and Andersen, T. (2002). Light, nutrients, and p:c ratios in algae: grazer performance related to food quality and quantity. *Ecology* 83, 1886–1898. doi: 10.1890/0012-9658(2002)083[1886:LNAPCR]2.0.CO;2

Hoffmann, L. J., Peeken, I., and Lochte, K. (2007). Effects of iron on the elemental stoichiometry during EIFEX and in the diatoms *Fragilariopsis kerguelensis* and *Chaetoceros dichaeta. Biogeosciences* 4, 569–579. doi: 10.5194/bg-4-569-2007

Huot, Y., and Babin, M. (2010). *Overview of Fluorescence Protocols: Theory, Basic Concepts, and Practice.* Dordrecht: Springer, 31–74.

Jauffrais, T., Jesus, B., Méléder, V., Turpin, V., Russo, A. D. P. G., Raimbault, P., et al. (2016). Physiological and photophysiological responses of the benthic diatom *Entomoneis paludosa* (Bacillariophyceae) to dissolved inorganic and organic nitrogen in culture. *Mar. Biol.* 163:115. doi: 10.1007/s00227-016-2888-9

Kemp, A. E., Pike, J., Pearce, R. B., and Lange, C. B. (2000). The 'Fall dump' - A new perspective on the role of a 'shade flora' in the annual cycle of diatom production and export flux. *Deep Sea Res. Part II Top. Stud. Oceanogr.* 47, 2129–2154. doi: 10.1016/S0967-0645(00)00019-9

Kemp, A. E. S., Pearce, R. B., Grigorov, I., Rance, J., Lange, C. B., Quilty, P., et al. (2006). Production of giant marine diatoms and their export at oceanic frontal zones: implications for si and c flux from stratified oceans. *Glob. Biogeochem. Cycles* 20:GB4S04. doi: 10.1029/2006GB002698

Kepkay, P., Niven, S., and Jellett, J. (1997). Colloidal organic carbon and phytoplankton speciation during a coastal bloom. *J. Plankton Res.* 19, 369–389. doi: 10.1093/plankt/19.3.369

Kristiansen, S., Farbrot, T., and Naustvoll, L. J. (2001). Spring bloom nutrient dynamics in the Oslofjord. *Mar. Ecol. Prog. Ser.* 219, 41–49. doi: 10.3354/meps219041

Lacour, T., Larivière, J., and Babin, M. (2017). Growth, Chl *a* content, photosynthesis, and elemental composition in polar and temperate microalgae. *Limnol. Oceanogr.* 62, 43–58. doi: 10.1002/lno.10369

Lacour, T., Larivière, J., Ferland, J., Bruyant, F., Lavaud, J., and Babin, M. (2018). The role of sustained photoprotective non-photochemical quenching in low temperature and high light acclimation in the bloom-forming Arctic diatom *Thalassiosira gravida.* *Front. Mar. Sci.* 5:354. doi: 10.3389/fmars.2018.00354

Lalande, C., Nöthig, E.-M., and Fortier, L. (2019). Algal export in the Arctic Ocean in times of global warming. *Geophys. Res. Lett.* 46, 5959–5967. doi: 10.1029/2019GL083167

Leong, S. C. Y., Maekawa, M., and Taguchi, S. (2010). Carbon and nitrogen acquisition by the toxic dinoflagellate *Alexandrium tamarense* in response to different nitrogen sources and supply modes. *Harmful Algae* 9, 48–58. doi: 10.1016/j.hal.2009.07.003

Leu, E., Søreide, J., Hessen, D., Falk-Petersen, S., and Berge, J. (2011). Consequences of changing sea-ice cover for primary and secondary producers in the european arctic shelf seas: timing, quantity, and quality. *Prog. Oceanogr.* 90, 18–32. doi: 10.1016/j.pocean.2011.02.004

Levasseur, M., Thompson, P. A., and Harrison, P. J. (1993). Physiological acclimation of marine phytoplankton to different nitrogen sources. *J. Phycol.* 29, 587–595. doi: 10.1111/j.0022-3646.1993.00587.x

Lomas, M. W. (2004). Nitrate reductase and urease enzyme activity in the marine diatom *Thalassiosira weissflogii* (Bacillariophyceae): interactions among nitrogen substrates. *Mar. Biol.* 144, 37–44. doi: 10.1007/s00227-003-1181-x

Lomas, M. W., Baer, S. E., Acton, S., and Krause, J. W. (2019). Pumped up by the cold: elemental quotas and stoichiometry of cold-water diatoms. *Front. Mar. Sci.* 6:286. doi: 10.3389/fmars.2019.00286

Lomas, M. W., and Krause, J. W. (2019). *Elemental Quotas and Stoichiometry of Polar Diatoms, United States, Antarctica, Baffin Bay, and Norway, 2016-2018.* Technical report, Arctic Data Center.

MacIntyre, H. L., and Cullen, J. J. (2005). "Using cultures to investigate the physiological ecology of microalgae," in *Algal Culturing Techniques,* ed R. A. Andersen (Amsterdam: Elsevier Academic Press), 287–326.

Macintyre, H. L., Kana, T. M., Anning, T., and Geider, R. J. (2002). Photoacclimation of photosynthesis irradiance response curves and photosynthetic pigments in microalgae and cyanobacteria. *J. Phycol.* 38, 17–38. doi: 10.1046/j.1529-8817.2002.00094.x

Martin, J., Dumont, D., and Tremblay, J.-É. (2013). Contribution of subsurface chlorophyll maxima to primary production in the coastal Beaufort Sea (Canadian Arctic): a model assessment. *J. Geophys. Res. Oceans* 118, 5873–5886. doi: 10.1002/2013JC008843

Martin, J., Tremblay, J.-É., Gagnon, J., Tremblay, G., Lapoussière, A., Jose, C., et al. (2010). Prevalence, structure and properties of subsurface chlorophyll maxima in canadian arctic waters. *Mar. Ecol. Prog. Ser.* 412, 69–84. doi: 10.3354/meps08666

Martin, J., Tremblay, J.-É., and Price, N. M. (2012). Nutritive and photosynthetic ecology of subsurface chlorophyll maxima in Canadian Arctic waters. *Biogeosciences* 9, 5353–5371. doi: 10.5194/bg-9-5353-2012

Martin-Jezequel, V., Hildebrand, M., and Brzezinski, M. A. (2000). Silicon metabolism in diatoms: implications for growth. *J. Phycol.* 36, 821–840. doi: 10.1046/j.1529-8817.2000.00019.x

Martiny, A. C., Pham, C. T., Primeau, F. W., Vrugt, J. A., Moore, J. K., Levin, S. A., et al. (2013a). Strong latitudinal patterns in the elemental ratios of marine plankton and organic matter. *Nat. Geosci.* 6, 279–283. doi: 10.1038/ngeo1757

Martiny, A. C., Vrugt, J. A., Primeau, F. W., and Lomas, M. W. (2013b). Regional variation in the particulate organic carbon to nitrogen ratio in the surface ocean. *Glob. Biogeochem. Cycles* 27, 723–731. doi: 10.1002/gbc.20061

McClelland, J. W., Holmes, R. M., Dunton, K. H., and Macdonald, R. W. (2012). The Arctic ocean estuary. *Estuar. Coasts* 35, 353–368. doi: 10.1007/s12237-010-9357-3

McLaughlin, F. A., and Carmack, E. C. (2010). Deepening of the nutricline and chlorophyll maximum in the Canada Basin interior, 2003–2009. *Geophys. Res. Lett.* 37:L24602. doi: 10.1029/2010GL045459

Morgan-Kiss, R. M., Priscu, J. C., Pocock, T., Gudynaite-Savitch, L., and Huner, N. P. A. (2006). Adaptation and acclimation of photosynthetic microorganisms to permanently cold environments. *Microbiol. Mol. Biol. Rev.* 70, 222–252. doi: 10.1128/MMBR.70.1.222-252.2006

Muggli, D. L., Lecourt, M., and Harrison, P. J. (1996). Effects of iron and nitrogen source on the sinking rate, physiology and metal composition of an oceanic diatom from the subarctic Pacific. *Mar. Ecol. Prog. Ser.* 132, 215–227. doi: 10.3354/meps132215

Mulholland, M. R., and Lomas, M. W. (2008). "Chapter 7 - Nitrogen uptake and assimilation," in *Nitrogen in the Marine Environment, 2nd Edn.*, eds D. G. Capone, D. A. Bronk, M. R. Mulholland, and E. J. Carpenter (San Diego, CA: Academic Press), 303–384.

Nummelin, A., Li, C., and Smedsrud, L. H. (2015). Response of Arctic Ocean stratification to changing river runoff in a column model. *J. Geophys. Res. Oceans* 120, 2655–2675. doi: 10.1002/2014JC010571

Overland, J. E., Wang, M., Walsh, J. E., and Stroeve, J. C. (2014). Future Arctic climate changes: adaptation and mitigation time scales. *Earths Future* 2, 68–74. doi: 10.1002/2013EF000162

Paasche, E. (1980). Silicon content of five marine plankton diatom species measured with a rapid filter method. *Limnol. Oceanogr.* 25, 474–480. doi: 10.4319/lo.1980.25.3.0474

Parsons, T. R., Maita, Y., and Lalli, C. M. (1984). *A Manual of Chemical & Biological Methods for Seawater Analysis.* Amsterdam: Pergamon.

Price, N. M. (2005). The elemental stoichiometry and composition of an iron-limited diatom. *Limnol. Oceanogr.* 50, 1159–1171. doi: 10.4319/lo.2005.50.4.1159

Price, N. M., and Harrison, P. J. (1988). Uptake of urea C and urea N by the coastal marine diatom *Thalassiosira pseudonana.* *Limnology and Oceanography* 33, 528–537. doi: 10.4319/lo.1988.33.4.0528

R Development Core Team (2019). *R: A Language and Environment for Statistical Computing.* Vienna: R Foundation for Statistical Computing.

Ruan, Z. and Giordano, M. (2017). The use of NH_4^+ rather than NO_3^- affects cell stoichiometry, C allocation, photosynthesis and growth in the cyanobacterium *Synechococcus* sp. UTEX LB 2380, only when energy is limiting. *Plant Cell Environ.* 40, 227–236. doi: 10.1111/pce.12858

Sarthou, G., Timmermans, K. R., Blain, S., and Tréguer, P. (2005). Growth physiology and fate of diatoms in the ocean: a review. *J. Sea Res.* 53, 25–42. doi: 10.1016/j.seares.2004.01.007

Shi, D., Li, W., Hopkinson, B. M., Hong, H., Li, D., Kao, S.-J., et al. (2015). Interactive effects of light, nitrogen source, and carbon dioxide on energy metabolism in the diatom *Thalassiosira pseudonana.* *Limnol. Oceanogr.* 60, 1805–1822. doi: 10.1002/lno.10134

Sieracki, M. E., Gifford, D. J., Gallager, S. M., and Davis, C. S. (1998). Ecology of a *Chaetoceros socialis* lauder patch on georges bank: distribution, microbial associations, and grazing losses. *Oceanography* 11, 30–35. doi: 10.5670/oceanog.1998.12

Simpson, K. G., Tremblay, J.-É., Brugel, S., and Price, N. M. (2013). Nutrient dynamics in the western canadian arctic. II. Estimates of new and regenerated production over the mackenzie shelf and cape bathurst polynya. *Mar. Ecol. Prog. Ser.* 484, 47–62. doi: 10.3354/meps10298

Simpson, K. G., Tremblay, J.-É., Gratton, Y., and Price, N. M. (2008). An annual study of inorganic and organic nitrogen and phosphorus and silicic acid in the southeastern Beaufort Sea. *J. Geophys. Res.* 113:C07016. doi: 10.1029/2007JC004462

Solôrzano, L., and Sharp, J. H. (1980). Determination of total dissolved phosphorus and particulate phosphorus in natural waters. *Limnol. Oceanogr.* 25, 754–758. doi: 10.4319/lo.1980.25.4.0754

Solomon, C. M., Collier, J. L., Berg, G. M., and Glibert, P. M. (2010). Role of urea in microbial metabolism in aquatic systems: a biochemical and molecular review. *Aquat. Microb. Ecol.* 59, 67–88. doi: 10.3354/ame01390

Spilling, K., Ylöstalo, P., Simis, S., and Seppälä, J. (2015). Interaction effects of light, temperature and nutrient limitations (N, P and Si) on growth, stoichiometry and photosynthetic parameters of the cold-water diatom *Chaetoceros wighamii*. *PLOS ONE* 10:e0126308. doi: 10.1371/journal.pone.0126308

Sterner, R. W., and Elser, J. J. (2002). *Ecological Stoichiometry the Biology of Elements from Molecules to the Biosphere*. Princeton, NJ: Princeton University Press.

Thompson, P. A., Levasseur, M. E., and Harrison, P. J. (1989). Light-limited growth on ammonium vs. nitrate: what is the advantage for marine phytoplankton? *Limnol. Oceanogr.* 34, 1014–1024. doi: 10.4319/lo.1989.34.6.1014

Tong, S., Hutchins, D. A., Fu, F., and Gao, K. (2016). Effects of varying growth irradiance and nitrogen sources on calcification and physiological performance of the coccolithophore *Gephyrocapsa oceanica* grown under nitrogen limitation. *Limnol. Oceanogr.* 61, 2234–2242. doi: 10.1002/lno.10371

Torres-Valdés, S., Tsubouchi, T., Bacon, S., Naveira-Garabato, A. C., Sanders, R., McLaughlin, F. A., et al. (2013). Export of nutrients from the Arctic Ocean. *J. Geophys. Res. Oceans* 118, 1625–1644. doi: 10.1002/jgrc.20063

Toseland, A., Daines, S. J., Clark, J. R., Kirkham, A., Strauss, J., Uhlig, C., et al. (2013). The impact of temperature on marine phytoplankton resource allocation and metabolism. *Nat. Clim. Change* 3, 979–984. doi: 10.1038/nclimate1989

Tréguer, P., Bowler, C., Moriceau, B., Dutkiewicz, S., Gehlen, M., Aumont, O., et al. (2018). Influence of diatom diversity on the ocean biological carbon pump. *Nat. Geosci.* 11, 27–37. doi: 10.1038/s41561-017-0028-x

Tremblay, J.-É., Anderson, L. G., Matrai, P., Coupel, P., Bélanger, S., Michel, C., et al. (2015). Global and regional drivers of nutrient supply, primary production and co2 drawdown in the changing arctic ocean. *Prog. Oceanogr.* 139, 171–196. doi: 10.1016/j.pocean.2015.08.009

Tremblay, J.-É., and Gagnon, J. (2009). "The effects of irradiance and nutrient supply on the productivity of arctic waters: a perspective on climate change," in *Influence of Climate Change on the Changing Arctic and Sub-Arctic Conditions*, eds J. C. J. Nihoul and A. G. Kostianoy (Dordrecht: Springer), 73–93.

Tremblay, J.-É., Gratton, Y., Fauchot, J., and Price, N. M. (2002). Climatic and oceanic forcing of new, net, and diatom production in the North Water. *Deep Sea Res. Part II Top. Stud. Oceanogr.* 49, 4927–4946. doi: 10.1016/S0967-0645(02)00171-6

Tremblay, J.-É., Raimbault, P., Garcia, N., Lansard, B., Babin, M., and Gagnon, J. (2014). Impact of river discharge, upwelling and vertical mixing on the nutrient loading and productivity of the Canadian Beaufort Shelf. *Biogeosciences* 11, 4853–4868. doi: 10.5194/bg-11-4853-2014

Tremblay, J.-É., Simpson, K., Martin, J., Miller, L., Gratton, Y., Barber, D., et al. (2008). Vertical stability and the annual dynamics of nutrients and chlorophyll fluorescence in the coastal, southeast Beaufort Sea. *J. Geophys. Res. Oceans* 113:C07S90. doi: 10.1029/2007JC004547

Wassmann, P., Duarte, C. M., Agustí, S., and Sejr, M. K. (2011). Footprints of climate change in the Arctic marine ecosystem. *Glob. Change Biol.* 17, 1235–1249. doi: 10.1111/j.1365-2486.2010.02311.x

Wassmann, P., and Reigstad, M. (2011). Future Arctic ocean seasonal ice zones and implications for Pelagic-Benthic coupling. *Oceanography* 24, 220–231. doi: 10.5670/oceanog.2011.74

Wheeler, B., and Torchiano, M. (2016). *lmPerm: Permutation Tests for Linear Models*. R package version 1.1-2.

Yamamoto-Kawai, M., Carmack, E., and McLaughlin, F. (2006). Nitrogen balance and arctic throughflow. *Nature* 443, 43–43. doi: 10.1038/443043a

Yamamoto-Kawai, M., McLaughlin, F. A., Carmack, E. C., Nishino, S., Shimada, K., and Kurita, N. (2009). Surface freshening of the Canada Basin, 2003–2007: river runoff versus sea ice meltwater. *J. Geophys. Res. Oceans* 114:C00A05. doi: 10.1029/2008JC005000

Young, J. N., Goldman, J. A. L., Kranz, S. A., Tortell, P. D., and Morel, F. M. M. (2015). Slow carboxylation of rubisco constrains the rate of carbon fixation during antarctic phytoplankton blooms. *New Phytol.* 205, 172–181. doi: 10.1111/nph.13021

Yvon-Durocher, G., Dossena, M., Trimmer, M., Woodward, G., and Allen, A. P. (2015). Temperature and the biogeography of algal stoichiometry. *Glob. Ecol. Biogeogr.* 24, 562–570. doi: 10.1111/geb.12280

Yvon-Durocher, G., Schaum, C.-E., and Trimmer, M. (2017). The Temperature Dependence of Phytoplankton Stoichiometry: Investigating the Roles of Species Sorting and Local Adaptation. *Front. Microbiol.* 8:2003. doi: 10.3389/fmicb.2017.02003